J. Math. Anal. Appl. 367 (2010) 116–128

Contents lists available at ScienceDirect

Journal of Mathematical Analysis and Applications

www.elsevier.com/locate/jmaa

Global stability of centrifugal filtration convection

S. Saravanan *, D. Brindha

Department of Mathematics, Bharathiar University, Coimbatore 641 046, Tamil Nadu, India

ARTICLE INFO

Article history:
Received 14 October 2009
Available online 21 December 2009
Submitted by B. Straughan

Keywords:
Nonlinear stability
Porous medium
Centrifugal force
Darcy's and Brinkman's equations

ABSTRACT

A nonlinear stability analysis is performed to study the onset of convection in a fluid saturated porous layer subject to alternating direction of the centrifugal body force. By introducing a suitable energy functional, the analysis is carried out for the Darcy and the Brinkman models of flow through porous media. The nonlinear result is unconditional and its sharpest limit is determined and is compared with the corresponding linear limit. The failure of linear theory in describing the instability is established in a certain region of the parameter space where possible subcritical instabilities may arise. The stability boundaries are discussed graphically for various values of the Darcy number and comparison is made with the available known results.

I. Introduction

Transport phenomena involving natural convection in rotating porous media are an intense field of research due to its applications in many areas like food processing, chemical processing, solidification and centrifugal casting of metals, rotating turbo-machinery, etc. In the study of rotating systems, inertial forces viz., centrifugal and Coriolis forces come into play in addition to the gravitational force. At high rotation speeds in the terrestrial environment thermal buoyancy can also be driven by the resulting centrifugal acceleration and dominates gravity induced buoyancy. This type of convection, referred to as centrifugal convection, is the only possibility if a system is rotating in zero-gravity condition. Centrifugal convection has received less attention when compared to gravitational convection, though there are many promising applications.

Vadasz [1] in his initial work dealt with a linear stability analysis to predict the onset of centrifugal convection in a porous medium governed by Darcy's law. He imposed conditions at the boundaries in such a way that the resulting temperature gradient is collinear with the centrifugal body force. Vadasz [2] then extended his previous analysis to know how the location of the axis about which the porous medium is being rotated affects the threshold representing the onset of centrifugal convection. He found an increase in both the critical centrifugal Rayleigh number, leading to unbounded Rc_{cr} and wavenumber as axis of rotation moves towards the hot boundary. Later Saravanan and Yamaguchi [3] studied centrifugal convection in a magnetic fluid filled differentially heated porous layer using linear stability analysis. They predicted two-dimensional flow pattern at the threshold and found that the magnetic field has a destabilising effect and can be suitably adjusted depending on particle magnetisation to enhance convection. Recently Om et al. [4] analysed the effect of rotation speed modulation on the onset of centrifugal convection using linear stability analysis and found that by applying modulation of proper frequency to the rotation speed, it is possible to delay or advance the onset of centrifugal convection.

Although linear theory does provide a useful result, in order to have a complete understanding one has to perform a nonlinear analysis which provides a threshold for global stability. Hence we shall carry out a nonlinear analysis of centrifugal convection which is not available in the literature till date. The approach adopted in the present article is by the application of energy method, pioneered by Serrin [5] and developed in its modern form by Straughan [6]. He emphasizes that the

* Corresponding author.
E-mail address: sshravan@lycos.com (S. Saravanan).

0022-247X/$ – see front matter
doi:10.1016/j.jmaa.2009.12.026

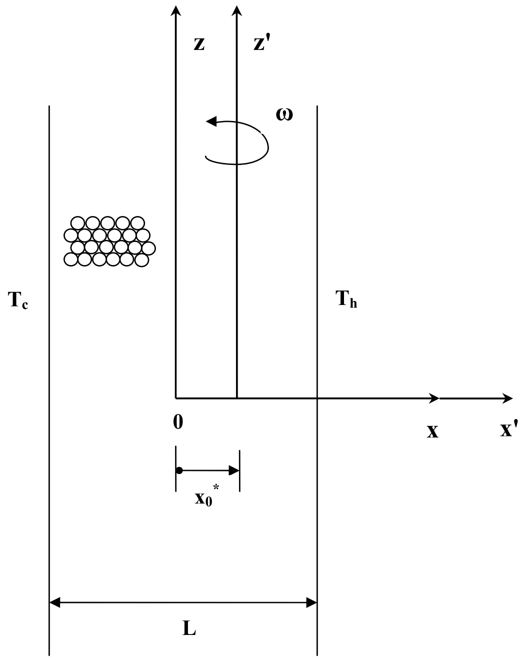

Fig. 1. A rotating fluid saturated porous layer having the rotation axis within its boundaries.

energy theory is certainly much stronger when the stability obtained is unconditional, i.e., for all initial data or for at least finite (nonvanishing) initial data. By introducing a coupling parameter in the energy method and by selecting it optimally, it is possible to sharpen the stability bound in many physical problems. The energy method has been applied to rotating fluid problems and results have been derived which are only conditional. However unconditional nonlinear results have been obtained for rotating porous systems. Straughan [7] obtained nonlinear energy results for thermal convection in a Darcian porous layer which is rotating about an axis orthogonal to the planes containing the layer. Lombardo and Mulone [8] attempted the same problem using the Brinkman model. Both of their results brought out the stabilising effect of rotation through sharp unconditional nonlinear energy stability results.

The purpose of the present paper is to study nonlinear stability of convective flow in a vertical rotating porous layer in the absence of gravity. We shall concentrate on convection induced by the centrifugal acceleration alone and neglect the Coriolis acceleration as done by Vadasz [1,2]. Both the Darcy and the Brinkman models are used and stress free as well as rigid boundaries are considered while employing the Brinkman model. Moreover the axis of rotation of the layer is assumed to be placed anywhere within the layer which leads to an alternating direction of the centrifugal body force.

II. Mathematical analysis

We consider a tall vertical fluid saturated porous layer $-L/2 < x < L/2$ of thickness L subject to a constant rotation rate ω about a vertical axis in a zero-gravity environment (see Fig. 1). The layer is heated on its right boundary (T_h), cooled on the left boundary (T_c) and as a result of these imposed thermal boundary conditions a uniform temperature gradient β is acting across the layer. This arrangement makes the centrifugal acceleration collinear with the temperature gradient. Free convection occurs as a result of the centrifugal body force. The axis of rotation is placed within the boundaries of the porous domain and at a dimensionless distance x_0 from the center of the layer. The offset distance is presented in a dimensionless form representing the ratio between the dimensional offset distance and the thickness of the porous layer in the form $x_0 = x_0^*/L$. The Coriolis effect is considered negligible. A partial justification for this was given by Govender [9] for the Darcy model using linear theory. The only inertial effect considered is the centrifugal acceleration, as far as the changes in density are concerned. The Boussinesq approximation is employed to account for the effects of the density variations. The layer is assumed to be narrow in the y-direction so that the y-component of centrifugal acceleration may be neglected.

1. The Darcy model

Assuming that the flow in the porous layer is according to Darcy's law, the complete system of dimensional equations for continuity, momentum and energy in the porous medium is

$$\nabla \cdot \bar{v} = 0$$

$$\frac{\mu}{k_p}\bar{v} = -\nabla p + \rho\omega^2(x - x_0)\hat{i}$$
$$\frac{\partial T}{\partial t} + (\bar{v}.\nabla)T = k_T\nabla^2 T \tag{1}$$

Here $\bar{v}$ is the filtration velocity, μ the dynamic viscosity of the fluid, k_p the permeability of porous medium, p the pressure, ρ the fluid density, $\hat{i}$ the unit vector in the x-direction, x_0 is the dimensionless offset distance from the rotation center, t the time, T the temperature and k_T the thermal conductivity of the fluid. In Eq. $(1)_2$, we have used the viscous term $\mu\bar{v}/k_p$ which is the usual Darcy term. The density ρ of fluids is, in general, a decreasing function of temperature T and hence the equation of state is given by

$$\rho(T) = \rho_0\big(1 - \alpha(T - T_0)\big) \tag{2}$$

where ρ_0 is the reference density, $T_0 = (T_c + T_h)/2$ the average temperature and α the coefficient of thermal expansion of the fluid.

Under this set up the governing equations (1) admit a basic quiescent state

$$\bar{v}_b = (0, 0, 0); \qquad T_b(x) = \beta x + T_0 \tag{3}$$

Its stability is now investigated by introducing a perturbation to this steady state, such that

$$(\bar{v}, p, T) = (\bar{v}_b, p_b, T_b) + \big(\bar{v}', p', T'\big) \tag{4}$$

where the primed quantities denote the disturbances on the corresponding terms. Upon substitution of (4) into (1) the governing equations for the disturbances may be written as

$$\nabla\cdot\bar{v} = 0$$
$$\frac{\mu}{k_p}\bar{v} + \rho_0\alpha T\omega^2(x - x_0)\hat{i} = -\nabla p$$
$$\frac{\partial T}{\partial t} + (\bar{v}_b.\nabla)T + (\bar{v}.\nabla)T_b + (\bar{v}.\nabla)T = k_T\nabla^2 T \tag{5}$$

after omitting the primes. Now we introduce the scales L for length, L^2/ν for time, ν/L for velocity, $\beta\nu L/k_T$ for temperature and $\mu\nu/k_p$ for pressure. Then the perturbed nondimensional equations governing convection are

$$\nabla\cdot\bar{v} = 0$$
$$\bar{v} + Rc\,T(x - x_0)\hat{i} = -\nabla p$$
$$Pr\frac{\partial T}{\partial t} + Pr(\bar{v}.\nabla)T = -v_x + \nabla^2 T \tag{6}$$

The nondimensional parameters appearing in (6) are $Rc = \alpha\beta\omega^2 k_p L^3/\nu k_T$, the centrifugal Rayleigh number and $Pr = \nu/k_T$, the Prandtl number. The above equations are supplemented with the conditions corresponding to impermeable and isothermal boundaries:

$$v_x = T = 0, \quad \text{on } x = \pm\frac{1}{2} \tag{7}$$

1.1. Linear instability analysis

The linearised equations are derived from system (6) by discarding the nonlinear terms and assuming a temporal growth rate of disturbances in the form

$$\bar{v}(x,z,t) = \bar{v}(x,z)e^{\sigma t}; \qquad T(x,z,t) = T(x,z)e^{\sigma t}; \qquad p(x,z,t) = p(x,z)e^{\sigma t} \tag{8}$$

where σ is a complex constant. It is important to note that the linear analysis approach assumes that the perturbation is small and so neglects terms of quadratic and higher order. Hence, the resulting system obtained by substituting (8) into (6), is

$$\nabla\cdot\bar{v} = 0$$
$$\bar{v} = -Rc\,T(x - x_0)\hat{i} - \nabla p$$
$$\sigma\,Pr\,T = \nabla^2 T - v_x \tag{9}$$

The principle of exchange of stabilities can be shown to be valid for this set up (see Appendix A), i.e., the possibility of the existence of over-stable motion is ruled out. It is well known that linear analysis often provides little information on the behaviour of nonlinear systems. Hence in such cases only instability can be deduced from the linear thresholds, as any potential growth in the nonlinear terms is not considered. Thus substituting $\sigma = 0$ in (9) we have the equations which govern the boundary for linearised instability, i.e.,

$$\begin{aligned} &\nabla \cdot \bar{v} = 0 \\ &\bar{v} + Rc\, T(x - x_0)\hat{i} = -\nabla p \\ &\nabla^2 T - v_x = 0 \end{aligned} \tag{10}$$

Let us denote the lowest eigenvalue for (10) together with the associated boundary conditions by Rc_L. In particular the linearised equations do not yield any information on global stability. It is, in general, possible for the solution of the full nonlinear equations (6) to become unstable at a value of Rc lower than Rc_L, and in this case subcritical instabilities occur. Exploring a nonlinear energy analysis provides thresholds for global stability.

To solve the above system numerically we first remove the pressure term by operating curl and then by introducing stream function $\Psi(x, z)$ we derive the eigenvalue equations

$$\begin{aligned} &D^2 U = k^2 U + Rc_L\, \Theta ik(x - x_0) \\ &D^2 \Theta = k^2 \Theta - Rc_L\, U ik(x - x_0) \end{aligned} \tag{11}$$

where $\Psi(x, z) = U(x)e^{ikz}$, $T(x, z) = \Theta(x)e^{ikz}$ are the normal modes, k is the wavenumber and $D = d/dx$. The relevant boundary conditions are

$$U = \Theta = 0 \quad \text{at } x = \pm\frac{1}{2} \tag{12}$$

Eqs. (11) and (12) constitute an eigenvalue system of equations for the linear centrifugal Rayleigh number Rc_L. In the numerical calculations we determine the critical linear centrifugal Rayleigh number as

$$Rc_{L,cr} = \min_k Rc_L(k)$$

1.2. Nonlinear stability analysis

Adopting the standard nonlinear energy approach in the stability measure $L^2(\Omega)$, we first multiply Eqs. $(6)_2$ and $(6)_3$ by $\bar{v}$ and T respectively, and integrate over Ω to obtain

$$\begin{aligned} &\|\bar{v}\|^2 = -Rc \int_\Omega (x - x_0) T v_x \, d\Omega \\ &Pr \frac{d}{dt}\frac{1}{2}\|T\|^2 = -\int_\Omega T v_x \, d\Omega - \|\nabla T\|^2 \end{aligned} \tag{13}$$

Here $\int_\Omega (\cdot)\, d\Omega$ denotes the integration over Ω and $\|\cdot\|$ denotes the $L^2(\Omega)$ norm, where Ω denotes a typical periodicity cell.

In order to study the nonlinear stability of the basic state, a kinetic like energy $E(t) = \frac{\xi Pr}{2}\|T(t)\|^2$ is constructed using Eqs. $(13)_{1,2}$ and its evolution is given by

$$\frac{dE}{dt} = Rc\mathcal{I} - \mathcal{D} \tag{14}$$

where

$$\begin{aligned} &\mathcal{I} = -\int_\Omega \left(x - x_0 + \frac{\xi}{Rc}\right) T v_x \, d\Omega \\ &\mathcal{D} = \|\bar{v}\|^2 + \xi \|\nabla T\|^2 \end{aligned}$$

with a coupling parameter ξ.

The idea is now to optimize an inequality involving the right hand side of (14). Hence, we define Rc_N by

$$\frac{1}{Rc_N} = \max_{\mathcal{H}} \frac{\mathcal{I}}{\mathcal{D}} \tag{15}$$

where $\mathcal{H}$ is the space of admissible functions to system (8) such that $\bar{v} \in L^2(\Omega), T \in H^1(\Omega)$, and $\bar{v} = 0$, $T = 0$, on $x = \pm\frac{1}{2}$. In this way we find from (14)

$$\frac{dE}{dt} \leqslant Rc\,\mathcal{D}\left(\max_{\mathcal{H}} \frac{\mathcal{I}}{\mathcal{D}}\right) - \mathcal{D}$$
$$= -\mathcal{D}\left(\frac{Rc_N - Rc}{Rc_N}\right)$$

The nonlinear stability threshold is now given by the variational problem (15).

1.3. Variational problem

The approach with nonlinear energy stability calculations is to find a variational problem like (15), determine the Euler–Lagrange equations and maximize the coupling parameter ξ to obtain the best value of Rc_N. We first redefine T as $T^\dagger = \sqrt{\xi}T$ to remove ξ from the denominator in (15). Thus

$$\frac{1}{Rc_N} = \max_{\mathcal{H}} \frac{-\int_\Omega f(x,\xi) T^\dagger v_x \, d\Omega}{\|\bar{v}\|^2 + \|\nabla T^\dagger\|^2} = \max_{\mathcal{H}} \frac{\mathcal{I}}{\mathcal{D}}$$

where $f(x,\xi) = (x - x_0 + \frac{\xi}{Rc})/\sqrt{\xi}$. The Euler–Lagrange equations for (15) are determined from

$$Rc_N\,\delta\mathcal{I} - \delta\mathcal{D} = 0$$

where

$$\delta\mathcal{I} = -\int_\Omega f(x,\xi)\frac{d}{d\epsilon}\left[\left(T^\dagger + \epsilon k\right)(v_x + \epsilon h_x)\right]_{\epsilon=0} d\Omega$$
$$= -\int_\Omega f(x,\xi)\left[T^\dagger h_x + v_x k\right] d\Omega$$

and

$$\delta\mathcal{D} = \int_\Omega \frac{d}{d\epsilon}\left[(\bar{v} + \epsilon\bar{h})^2 + \left(\nabla\left(T^\dagger + \epsilon k\right)\right)^2\right]_{\epsilon=0} d\Omega$$
$$= 2\int_\Omega \bar{v}\cdot\bar{h}\,d\Omega - 2\int_\Omega k\nabla^2 T^\dagger\,d\Omega$$

This leads to the Euler–Lagrange equations

$$\begin{aligned} &\nabla\cdot\bar{v} = 0 \\ &\bar{v} + \frac{1}{2}Rc_N\,f(x,\xi)T^\dagger\hat{i} = -\nabla\pi \\ &\nabla^2 T^\dagger - \frac{1}{2}Rc_N\,f(x,\xi)v_x = 0 \end{aligned} \tag{16}$$

with the appropriate boundary conditions where π is a multiplier.

Now we obtain the eigenvalue equations by introducing stream function $\Psi(x,z)$ as

$$\begin{aligned} &D^2U = k^2U + \frac{(Rc_N\,fik\sqrt{\xi}\,)}{2}\Theta \\ &D^2\Theta = k^2\Theta - \frac{(Rc_N\,fik)}{2\sqrt{\xi}}U \end{aligned} \tag{17}$$

where the normal modes are as defined earlier. Here k is the wavenumber and $D = d/dx$. The relevant boundary conditions are

$$U = \Theta = 0 \quad \text{at}\ x = \pm\frac{1}{2} \tag{18}$$

Eqs. (17) and (18) constitute an eigenvalue system of equations for the nonlinear centrifugal Rayleigh number Rc_N. The 'energy' parameter ξ must be chosen to make Rc_N as large as possible. Hence we calculate the critical nonlinear centrifugal Rayleigh number by the optimization:

$$Rc_{N,cr} = \max_{\xi>0}\min_{k} Rc_N(k,\xi)$$

2. The Brinkman model

Eqs. (1) are appropriate only if the motion is sufficiently slow and the porosity is not close to unity. If account is taken of the boundary layer effect which arises near a boundary and the effect of inertial terms which becomes significant at high velocities, extensions of Darcy's law must be considered. When the porosity is sufficiently large, then it is appropriate to use Brinkman's equation (see [10]). Accordingly the viscous resistance $\lambda\nabla^2\bar{v}$ is added to the RHS of Eq. $(1)_2$, Eqs. $(1)_1$, $(1)_3$, (2) remain the same, where λ is the effective viscosity. The newly added Laplacian term is important in the region near the boundaries. These equations also admit a steady basic state of the form (3). The corresponding perturbed quantities satisfy the equations

$$\begin{aligned}
&\nabla\cdot\bar{v}=0\\
&\frac{\mu}{k_p}\bar{v}+\rho_0\alpha T\omega^2(x-x_0)\hat{i}=-\nabla p+\lambda\nabla^2\bar{v}\\
&\frac{\partial T}{\partial t}+(\bar{v}.\nabla)T=-\beta v_x+k_T\nabla^2 T
\end{aligned}$$

where the primes have been omitted for convenience. These equations are then nondimensionalized using the scales defined in the previous section which result in

$$\begin{aligned}
&\nabla\cdot\bar{v}=0\\
&\bar{v}+Rc\,T(x-x_0)\hat{i}=-\nabla p+Da\,\nabla^2\bar{v}\\
&Pr\frac{\partial T}{\partial t}+Pr(\bar{v}.\nabla)T=-v_x+\nabla^2 T
\end{aligned}\tag{19}$$

where $Da=\lambda k_p/(\mu L^2)$, the Darcy number. The boundaries remain isothermal as in the Darcy model whereas we consider two types of velocity boundary conditions, viz., stress free boundaries in which the boundaries are flat and no tangential stresses act and rigid boundaries in which all components of velocity vanish. These lead to the nondimensional boundary conditions

$$\begin{aligned}
&v_x=Dv_x=T=0,\quad \text{on } x=\pm\frac{1}{2}\quad \text{for rigid boundaries}\\
&v_x=D^2v_x=T=0,\quad \text{on } x=\pm\frac{1}{2}\quad \text{for stress free boundaries}
\end{aligned}$$

where $D\equiv d/dx$.

2.1. Linear instability analysis

Firstly we note that the linearised equations which follow from (19) by substituting (8) are

$$\begin{aligned}
&\nabla\cdot\bar{v}=0\\
&\bar{v}+Rc\,T(x-x_0)\hat{i}=-\nabla p+Da\,\nabla^2\bar{v}\\
&Pr\,\sigma T=-v_x+\nabla^2 T
\end{aligned}\tag{20}$$

When $\sigma=0$ at the marginal state, which is proved in Appendix A, we have

$$\begin{aligned}
&\nabla\cdot\bar{v}=0\\
&\bar{v}+Rc\,T(x-x_0)\hat{i}=-\nabla p+Da\,\nabla^2\bar{v}\\
&\nabla^2 T-v_x=0
\end{aligned}$$

Introducing the normal modes as earlier, we obtain the resultant equations as

$$\begin{aligned}
&Da\,D^4U=\big(2k^2\,Da+1\big)D^2U-\big(Da\,k^4+k^2\big)U-Rc_L(x-x_0)ik\Theta\\
&D^2\Theta=k^2\Theta-Rc_L\,Uik(x-x_0)
\end{aligned}\tag{21}$$

The relevant boundary conditions at $x=\pm\frac{1}{2}$ are

$$\begin{aligned}
&U=DU=\Theta=0,\quad \text{for rigid case}\\
&U=D^2U=\Theta=0,\quad \text{for stress free case}
\end{aligned}\tag{22}$$

The critical linear centrifugal Rayleigh number is then determined as

$$Rc_{L,cr}=\min_k Rc_L(k)$$

2.2. Nonlinear stability analysis

A nonlinear energy analysis may be developed as we did in the Darcy model. Multiplying $(19)_2$ and $(19)_3$ by $\bar{v}$ and T respectively, and integrating over Ω we find

$$\begin{aligned} \|\bar{v}\|^2 &= -Rc\int_\Omega T(x-x_0)v_x\,d\Omega - Da\,\|\nabla\bar{v}\|^2 \\ Pr\frac{d}{dt}\frac{1}{2}\|T\|^2 &= -\int_\Omega Tv_x\,d\Omega - \|\nabla T\|^2 \end{aligned} \tag{23}$$

For a positive coupling parameter $\xi^\dagger$, the evolution of the energy $E(t)=\frac{1}{2}Pr\,\xi^\dagger\|T\|^2$ is constructed using $(23)_{1,2}$ and (14), with

$$\begin{aligned} \mathcal{I} &= -\int_\Omega T^\dagger f\big(x,\xi^\dagger\big)v_x\,d\Omega \\ \mathcal{D} &= \|\bar{v}\|^2 + Da\,\|\nabla\bar{v}\|^2 + \big\|\nabla T^\dagger\big\|^2 \end{aligned}$$

where $f(x,\xi^\dagger)=(x-x_0+\frac{\xi^\dagger}{Rc})/\sqrt{\xi^\dagger}$, $T^\dagger=\sqrt{\xi^\dagger}T$. The Euler–Lagrange equations become

$$\begin{aligned} &\nabla\cdot\bar{v}=0 \\ &\bar{v}+\frac{1}{2}Rc_N\,fT^\dagger\hat{i} - Da\,\nabla^2\bar{v} = -\nabla\pi \\ &\nabla^2T^\dagger - \frac{1}{2}Rc_N\,fv_x = 0 \end{aligned} \tag{24}$$

where π is the Lagrange multiplier.

It is worth observing that Brinkman's equation reduces to Darcy's one as $Da\to 0$ and to a form of Navier–Stokes equation for fluids as $Da\to\infty$. Hence it is enough to consider the Euler–Lagrange equations found using the Brinkman model alone for further analysis.

In order to actually find the sharp limits we solve these Euler–Lagrange equations for Rc_N. After removing π by operating *curl* and with the use of stream functions $\Psi(x,z)$, Eqs. (24) may then be reduced to

$$\begin{aligned} Da\,D^4U &= \big(2k^2\,Da+1\big)D^2U - \big(Da\,k^4+k^2\big)U - \frac{(Rc_N\,fik\sqrt{\xi^\dagger})}{2}\Theta \\ D^2\Theta &= k^2\Theta - \frac{(Rc_N\,fik)}{2\sqrt{\xi^\dagger}}U \end{aligned} \tag{25}$$

where $\Psi(x,z)=U(x)e^{ikz}$ and $T(x,z)=\Theta(x)e^{ikz}$ in which k is the wavenumber. Eqs. (25) together with (22) constitute an eigenvalue system of equations for the nonlinear centrifugal Rayleigh number Rc_N. In the numerical calculations we determine the critical centrifugal Rayleigh number as

$$Rc_{N,cr} = \max_{\xi^\dagger>0}\min_k Rc_N\big(\xi^\dagger,k\big) \tag{26}$$

III. Numerical technique

The linear and nonlinear critical values are found using compound matrix method [11] which is superior than the other methods of its kind. The idea of using compound matrices was stimulated initially by the need to overcome certain difficulties which arose in the asymptotic theory of eigenvalue problems. It soon became evident, however, that they also provide a simple and effective method for the numerical treatment of eigenvalue problems for stiff differential equations, especially those of hydrodynamic type which are typically of order four or six [12]. Eigenvalue problems for ordinary differential equations are usually treated by first defining a solution matrix which satisfies certain prescribed initial conditions and the required eigenvalues are then obtained as the roots of some minor of the solution matrix. If we attempt to evaluate this minor by computing its elements separately, as in a standard shooting method, then there may be a serious loss of numerical accuracy especially when the differential equation is stiff. This difficulty can be avoided, however, by considering the differential equation satisfied by a certain compound matrix whose elements are the minors of the solution matrix, and in this way we can compute the required minor directly.

We shall describe this method to solve (25) and (22). Accordingly we define

$$\mathbf{U}_1 = \left(U_1, U_1', U_1'', U_1''', \Theta_1, \Theta_1'\right)^T$$
$$\mathbf{U}_2 = \left(U_2, U_2', U_2'', U_2''', \Theta_2, \Theta_2'\right)^T$$
$$\mathbf{U}_3 = \left(U_3, U_3', U_3'', U_3''', \Theta_3, \Theta_3'\right)^T$$

where $\mathbf{U}_i$, $i = 1, 2$ and 3 are independent solutions to the systems (25) and (22) for different initial values. In the case of rigid boundaries $(22)_1$ we choose $\mathbf{U}_1$, $\mathbf{U}_2$ and $\mathbf{U}_3$ to be solutions with starting values at $x = -\frac{1}{2}$ of $(0, 0, 1, 0, 0, 0)^T$, $(0, 0, 0, 1, 0, 0)^T$, and $(0, 0, 0, 0, 0, 1)^T$, respectively. In the stress free case $(22)_2$ we choose $\mathbf{U}_1$, $\mathbf{U}_2$ and $\mathbf{U}_3$ to start with $(0, 1, 0, 0, 0, 0)^T$, $(0, 0, 0, 1, 0, 0)^T$ and $(0, 0, 0, 0, 0, 1)^T$ respectively at $x = -\frac{1}{2}$.

We define $6C_3$ new variables y_1 to y_{20} as the 3×3 minors of the 6×6 solution matrix whose first, second and third columns are $\mathbf{U}_1$, $\mathbf{U}_2$ and $\mathbf{U}_3$ respectively. For example, we define

$$\begin{aligned} y_1 &= \begin{vmatrix} U_1 & U_2 & U_3 \\ U_1' & U_2' & U_3' \\ U_1'' & U_2'' & U_3'' \end{vmatrix} \\ &= U_1U_2'U_3'' + U_2U_3'U_1'' + U_3U_1'U_2'' - U_1U_3'U_2'' - U_2U_1'U_3'' - U_3U_2'U_1'' \end{aligned}$$

The idea is to define $y_2 - y_{20}$ similarly and then obtain differential equations for the y_i by differentiation. Thus, we write

$$\begin{aligned}
y_2 &= U_1U_2'U_3''' + U_2U_3'U_1''' + U_3U_1'U_2''' - U_1U_3'U_2''' - U_2U_1'U_3''' - U_3U_2'U_1''' \\
y_3 &= U_1U_2'\Theta_3 + U_2U_3'\Theta_1 + U_3U_1'\Theta_2 - U_1U_3'\Theta_2 - U_2U_1'\Theta_3 - U_3U_2'\Theta_1 \\
y_4 &= U_1U_2'\Theta_3' + U_2U_3'\Theta_1' + U_3U_1'\Theta_2' - U_1U_3'\Theta_2' - U_2U_1'\Theta_3' - U_3U_2'\Theta_1' \\
y_5 &= U_1U_2''U_3''' + U_2U_3''U_1''' + U_3U_1''U_2''' - U_1U_3''U_2''' - U_2U_1''U_3''' - U_3U_2''U_1''' \\
y_6 &= U_1U_2''\Theta_3 + U_2U_3''\Theta_1 + U_3U_1''\Theta_2 - U_1U_3''\Theta_2 - U_2U_1''\Theta_3 - U_3U_2''\Theta_1 \\
y_7 &= U_1U_2''\Theta_3' + U_2U_3''\Theta_1' + U_3U_1''\Theta_2' - U_1U_3''\Theta_2' - U_2U_1''\Theta_3' - U_3U_2''\Theta_1' \\
y_8 &= U_1U_2'''\Theta_3 + U_2U_3'''\Theta_1 + U_3U_1'''\Theta_2 - U_1U_3'''\Theta_2 - U_2U_1'''\Theta_3 - U_3U_2'''\Theta_1 \\
y_9 &= U_1U_2'''\Theta_3' + U_2U_3'''\Theta_1' + U_3U_1'''\Theta_2' - U_1U_3'''\Theta_2' - U_2U_1'''\Theta_3' - U_3U_2'''\Theta_1' \\
y_{10} &= U_1\Theta_2\Theta_3' + U_2\Theta_3\Theta_1' + U_3\Theta_1\Theta_2' - U_1\Theta_3\Theta_2' - U_2\Theta_1\Theta_3' - U_3\Theta_2\Theta_1' \\
y_{11} &= U_1'U_2''U_3''' + U_2'U_3''U_1''' + U_3'U_1''U_2''' - U_1'U_3''U_2''' - U_2'U_1''U_3''' - U_3'U_2''U_1''' \\
y_{12} &= U_1'U_2''\Theta_3 + U_2'U_3''\Theta_1 + U_3'U_1''\Theta_2 - U_1'U_3''\Theta_2 - U_2'U_1''\Theta_3 - U_3'U_2''\Theta_1 \\
y_{13} &= U_1'U_2''\Theta_3' + U_2'U_3''\Theta_1' + U_3'U_1''\Theta_2' - U_1'U_3''\Theta_2' - U_2'U_1''\Theta_3' - U_3'U_2''\Theta_1' \\
y_{14} &= U_1'U_2'''\Theta_3 + U_2'U_3'''\Theta_1 + U_3'U_1'''\Theta_2 - U_1'U_3'''\Theta_2 - U_2'U_1'''\Theta_3 - U_3'U_2'''\Theta_1 \\
y_{15} &= U_1'U_2'''\Theta_3' + U_2'U_3'''\Theta_1' + U_3'U_1'''\Theta_2' - U_1'U_3'''\Theta_2' - U_2'U_1'''\Theta_3' - U_3'U_2'''\Theta_1' \\
y_{16} &= U_1'\Theta_2\Theta_3' + U_2'\Theta_3\Theta_1' + U_3'\Theta_1\Theta_2' - U_1'\Theta_3\Theta_2' - U_2'\Theta_1\Theta_3' - U_3'\Theta_2\Theta_1' \\
y_{17} &= U_1''U_2'''\Theta_3 + U_2''U_3'''\Theta_1 + U_3''U_1'''\Theta_2 - U_1''U_3'''\Theta_2 - U_2''U_1'''\Theta_3 - U_3''U_2'''\Theta_1 \\
y_{18} &= U_1''U_2'''\Theta_3' + U_2''U_3'''\Theta_1' + U_3''U_1'''\Theta_2' - U_1''U_3'''\Theta_2' - U_2''U_1'''\Theta_3' - U_3''U_2'''\Theta_1' \\
y_{19} &= U_1''\Theta_2\Theta_3' + U_2''\Theta_3\Theta_1' + U_3''\Theta_1\Theta_2' - U_1''\Theta_3\Theta_2' - U_2''\Theta_1\Theta_3' - U_3''\Theta_2\Theta_1' \\
y_{20} &= U_1'''\Theta_2\Theta_3' + U_2'''\Theta_3\Theta_1' + U_3'''\Theta_1\Theta_2' - U_1'''\Theta_3\Theta_2' - U_2'''\Theta_1\Theta_3' - U_3'''\Theta_2\Theta_1'
\end{aligned} \tag{27}$$

By differentiating each y_i in turn and simplifying we arrive at the following differential equations for the y_i's:

$$\begin{aligned}
y_1' &= y_2 \\
y_2' &= y_5 + \frac{(2k^2\,Da+1)}{Da}y_1 - \frac{(Rc_N\,fik\sqrt{\xi^\dagger})}{2\,Da}y_3 \\
y_3' &= y_4 + y_6 \\
y_4' &= k^2y_3 + y_7 \\
y_5' &= y_{11} - \frac{(Rc_N\,fik\sqrt{\xi^\dagger})}{2\,Da}y_6
\end{aligned}$$

$$
\begin{aligned}
y_6' &= y_7 + y_8 + y_{12}\\
y_7' &= y_9 + k^2 y_6 + y_{13}\\
y_8' &= y_9 + \frac{(2k^2\,Da+1)}{Da} y_6 + y_{14}\\
y_9' &= \frac{(2k^2\,Da+1)}{Da} y_7 + k^2 y_8 - \frac{(Rc_N\, fik\sqrt{\xi^\dagger})}{2\,Da} y_{10} + y_{15}\\
y_{10}' &= y_{16}\\
y_{11}' &= -\frac{k^2(1+Da\,k^2)}{Da} y_1 - \frac{(Rc_N\, fik\sqrt{\xi^\dagger})}{2\,Da} y_{12}\\
y_{12}' &= y_{13} + y_{14}\\
y_{13}' &= -\frac{(Rc_N\, fik)}{2\sqrt{\xi^\dagger}} y_1 + k^2 y_{12} + y_{15}\\
y_{14}' &= \frac{k^2(1+Da\,k^2)}{Da} y_3 + \frac{(2k^2\,Da+1)}{Da} y_{12} + y_{15} + y_{17}\\
y_{15}' &= -\frac{(Rc_N\, fik)}{2\sqrt{\xi^\dagger}} y_2 + \frac{k^2(1+Da\,k^2)}{Da} y_4 + \frac{(2k^2\,Da+1)}{Da} y_{13} + k^2 y_{14} - \frac{(Rc_N\, fik\sqrt{\xi^\dagger})}{2\,Da} y_{16} + y_{18}\\
y_{16}' &= -\frac{(Rc_N\, fik)}{2\sqrt{\xi^\dagger}} y_3 + y_{19}\\
y_{17}' &= \frac{k^2(1+Da\,k^2)}{Da} y_6 + y_{18}\\
y_{18}' &= -\frac{Rc_N\, fik}{2\sqrt{\xi^\dagger}} y_5 + \frac{k^2(1+Da\,k^2)}{Da} y_7 + k^2 y_{17} - \frac{(Rc_N\, fik\sqrt{\xi^\dagger})}{2\,Da} y_{19}\\
y_{19}' &= -\frac{Rc_N\, fik}{2\sqrt{\xi^\dagger}} y_6 + y_{20}\\
y_{20}' &= -\frac{Rc_N\, fik}{2\sqrt{\xi^\dagger}} y_8 - \frac{k^2(1+Da\,k^2)}{Da} y_{10} + \frac{(2k^2\,Da+1)}{Da} y_{19}
\end{aligned}
\tag{28}
$$

From the initial conditions on $\mathbf{U}_i$ we see that the system (28) has to be integrated numerically from 0 to 1 with the initial condition

$$y_{18}\left(-\frac{1}{2}\right) = 1$$

for rigid boundaries. The appropriate final condition which satisfies $(22)_1$ is seen using (27) to be

$$y_3\left(\frac{1}{2}\right) = 0 \tag{29}$$

Similarly when the boundaries are stress free we have the initial condition

$$y_{15}\left(-\frac{1}{2}\right) = 1$$

and the final condition

$$y_6\left(\frac{1}{2}\right) = 0 \tag{30}$$

The eigenvalue Rc_N is varied until (29) or (30) is satisfied.

IV. Results and conclusion

In this section we present the linear and nonlinear limits graphically in terms of critical centrifugal Rayleigh number and critical wavenumber. We commence with the results when the axis of rotation is at the center of the porous layer (i.e. $x_0 = 0$). Fig. 2 shows the marginal curves, for different values of Da obtained by both linear and nonlinear analyses. These curves divide Rc–k plane into two regions, the region above the linear curves representing linearly unstable state

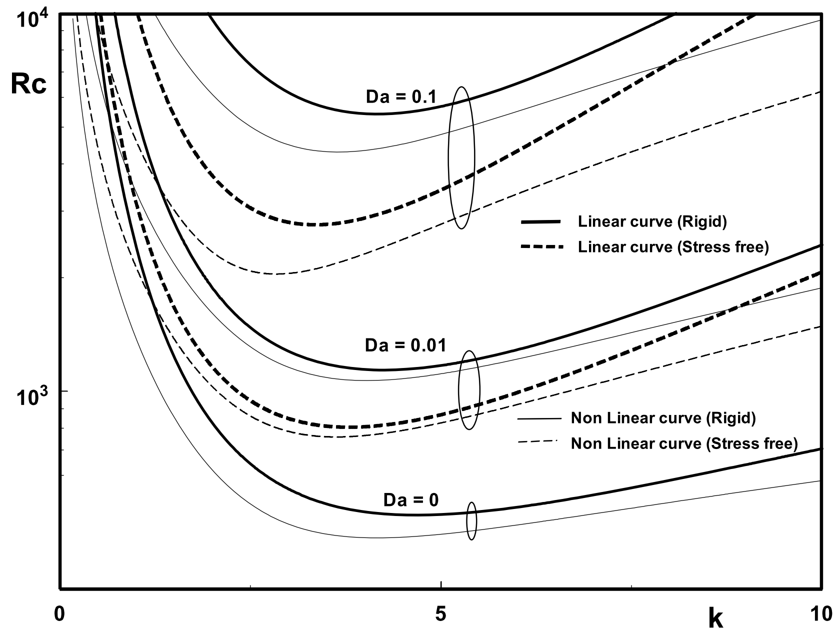

Fig. 2. Marginal curves of Rc when $x_0 = 0$.

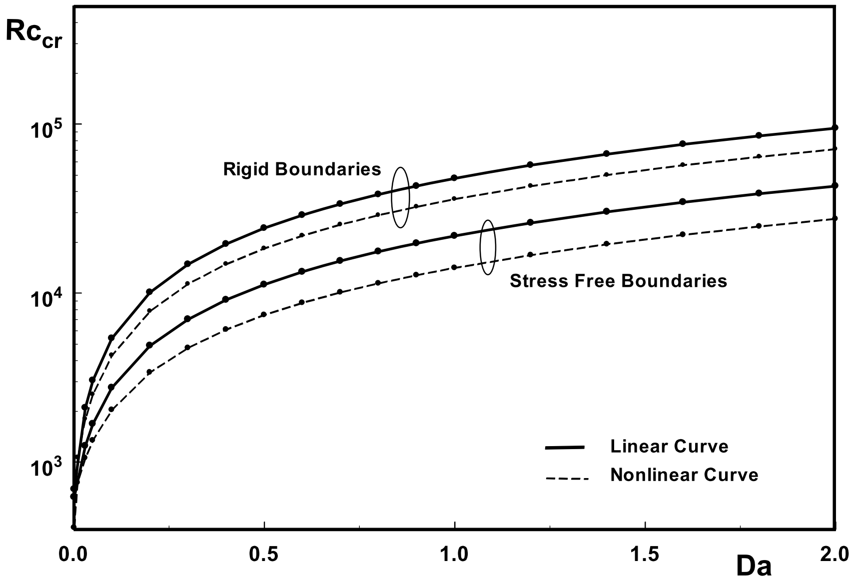

Fig. 3. Critical Rc against Da^* when $x_0 = 0$.

and the region below the nonlinear curves representing nonlinearly stable state. The minimum in each curve represents the critical centrifugal Rayleigh number and the corresponding wavenumber is the critical wavenumber. In the Darcy limit, corresponding to $Da = 0$, $Rc_{L,cr}$ becomes 471.19 with $k_{cr} = 4.68$. These values agree well with those for an analogous problem in a magnetic fluid saturated porous layer in the absence of magnetic field as discussed by Saravanan and Yamaguchi [3]. It is seen that the marginal curves depend strongly on Da and get displaced upwards as Da takes higher values. This is anticipated as the boundary layer thickness increases together with Da and causes the fluid to move with more resistance near the boundaries. In other words the onset of convection is delayed for an increase in Da. We also notice that the effect of Da is suppressed by the stress free boundaries when compared to the rigid boundaries. Moreover in Fig. 2 the nonlinear marginal curves are seen below the linear curves. This shows that the linear and nonlinear theories do not match proving that there are regions of subcritical instabilities where the stability behaviour cannot be predicted.

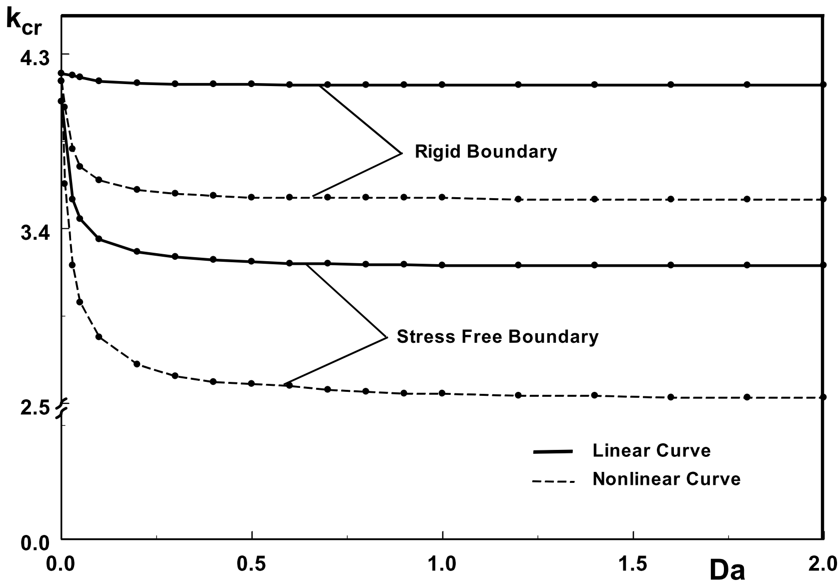

Fig. 4. Critical k against Da^* when $x_0 = 0$.

The variation of Rc_{cr} against Da is illustrated in Fig. 3 for both the rigid and stress free boundaries. In both cases Rc_{cr} rises and the increase is more for lower values of Da and becomes steady for higher values of Da. In particular it is found to obey the linear asymptotic law

$$Rc_{L,cr} = \begin{cases} 47073\,Da + 712 & \text{for rigid boundaries} \\ 21214\,Da + 657 & \text{for stress free boundaries} \end{cases}$$

$$Rc_{N,cr} = \begin{cases} 35258\,Da + 787 & \text{for rigid boundaries} \\ 13385\,Da + 750 & \text{for stress free boundaries} \end{cases}$$

as $Da \to \infty$. k_{cr} against Da for both the boundaries are depicted in Fig. 4 when $x_0 = 0$. It shows the appearance of bigger cells at the onset condition for the stress free boundaries with a sudden change in size as Da increases in the neighbourhood of $Da = 0$.

The results for Rc_{cr} against x_0 are presented in Fig. 5 in order to observe the effect of the shifting of the rotating axis on the critical values of Rc obtained by both the theories. For $x_0 = -0.5$ i.e., for a porous layer with its axis of rotation on the left wall, $Rc_{L,cr} = 77.10$ confirming excellently with $Rc_{L,cr} = 7.81\pi^2$ of Vadasz [1]. When $Da = 0$, $Rc_{L,cr}$ increases monotonically against x_0 and becomes unbounded as $x_0 \to 0.5$. One should keep in mind the underlying 'stable' configuration caused by the centrifugal force by pushing the denser fluid particles towards the left wall when $x_0 = 0.5$. For an increase in Da the same trend of critical Rayleigh number is maintained irrespective of the location of the rotating axis with an increased $Rc_{L,cr}$ and a stable no motion state occurs for a wide range of x_0 near $x_0 = 0.5$. The nonlinear limit agrees satisfactorily well with the linear one for $x_0 < -0.2$. But it deviates from the linear instability one as x_0 increases beyond -0.2. In fact $Rc_{N,cr}$ of the nonlinear theory remains finite for all values of x_0. Thus we may conclude that the nonlinear stability threshold does not match with the linear stability one in general. We again notice that this result is unconditional and delimits the region of subcritical bifurcations. This may be verified by performing a suitable experiment. Thus the energy method produces practically useful optimal results which cannot be determined by the linear theory.

The change in k_{cr} against location of the axis of rotation displayed in Fig. 6. The nonlinear results show that convection always sets in with a finite wavenumber in contrast to the linear theory which predicts the onset of convection with an unbounded wavenumber as $x_0 \to 0.5$. We note that the effect of Da on the size of convection cells at the threshold, obtained by nonlinear theory is prominent for all values of x_0 whereas that of linear theory is significant when x_0 is negative. It is also observed from both linear and nonlinear limits that the stress free boundaries augment the onset of instability via enhanced convective motion for all values of x_0.

Acknowledgments

The authors thank University Grants Commission, India for its support through DRS Special Assistance Programme in Fluid Dynamics. This work was carried out as a part of a research project (No. SR/FTP/MS-02/2007) awarded by SERC, Department of Science and Technology, India.

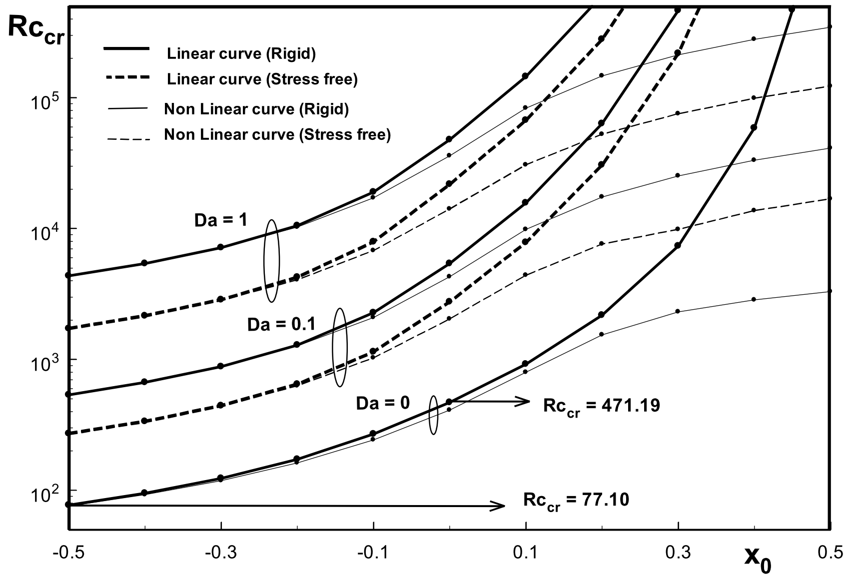

Fig. 5. Critical Rc against x_0.

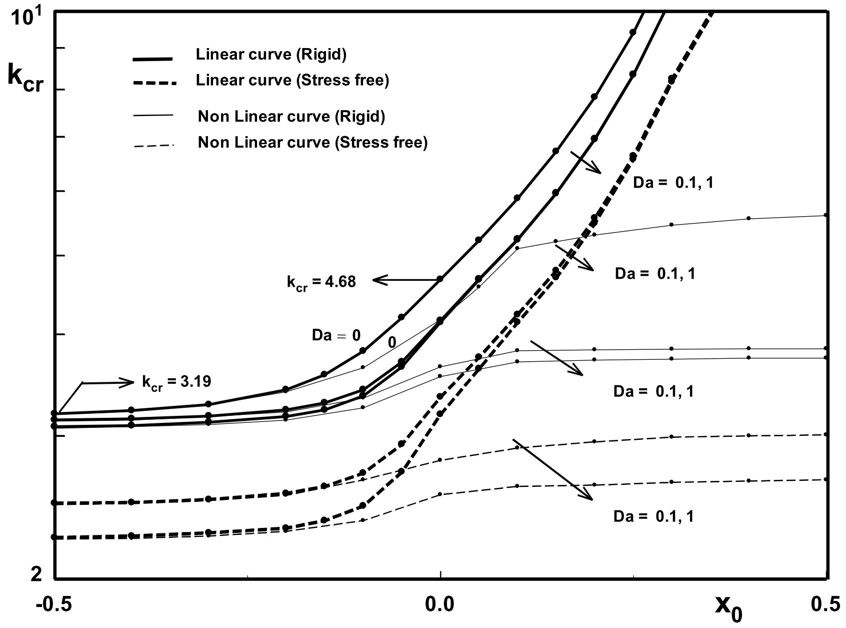

Fig. 6. Critical k against x_0.

Appendix A

Here we shall prove the principle of exchange of stabilities for the Brinkman model. Applying curl twice on $(20)_2$ and introducing the normal modes in the resulting equation and $(20)_3$ we obtain

$$\begin{aligned} &Da\,D^4U - \left(2k^2\,Da+1\right)D^2U + k^2\left(Da\,k^2+1\right)U + Rc\,k^2(x-x_0)\Theta = 0 \\ &\left(D^2 - \left(k^2 + Pr\,\sigma\right)\right)\Theta - U = 0 \end{aligned} \tag{31}$$

In particular when $Da = 0$ the equations are those of the Darcy model. These two equations can be combined into a single equation in Θ as

$$\begin{aligned} &\left\{Da\,D^6 - \left[Da\left(k^2+Pr\,\sigma\right) + \left(2k^2\,Da+1\right)\right]D^4 + \left[\left(2k^2\,Da+1\right)\left(k^2+Pr\,\sigma\right)\right.\right. \\ &\quad \left.\left. + k^2\left(Da\,k^2+1\right)\right]D^2 - k^2\left(Da\,k^2+1\right)\left(k^2+Pr\,\sigma\right)\right\}\Theta + Rc\,k^2(x-x_0)\Theta = 0 \end{aligned} \tag{32}$$

The boundary conditions $(22)_2$ in terms of Θ are

$$\Theta = D^2\Theta = D^4\Theta = 0$$

We now multiply (32) by Θ^*, the complex conjugate of Θ, and integrate over the layer we find, after using the boundary conditions corresponding to stress free boundaries,

$$-Da\langle|D^3\Theta|^2\rangle - [Da(k^2 + Pr\,\sigma) + (2k^2\,Da + 1)]\langle|D^2\Theta|^2\rangle - [(2k^2\,Da + 1)(k^2 + Pr\,\sigma) + k^2(Da\,k^2 + 1)]\langle|D\Theta|^2\rangle$$
$$- k^2(Da\,k^2 + 1)(k^2 + Pr\,\sigma)\langle|\Theta|^2\rangle + Rc\,k^2\langle(x - x_0)|\Theta|^2\rangle = 0$$

where $\langle\cdot\rangle$ is the usual integration with respect to x from $x = -\frac{1}{2}$ to $x = \frac{1}{2}$. The real and imaginary parts of the above equation must vanish separately and so letting $\sigma = \Re(\sigma) + i\Im(\sigma)$ and vanishing of the imaginary part gives

$$Pr\{Da\langle|D^2\Theta|^2\rangle + (2k^2\,Da + 1)\langle|D\Theta|^2\rangle + k^2(Da\,k^2 + 1)\langle|\Theta|^2\rangle\}\Im(\sigma) = 0$$

Hence,

$$\Im(\sigma) = 0$$

proving the principle of exchange of stabilities in the case of stress free boundary conditions.

In order to prove the principle for rigid boundaries, we follow the moment method as suggested by Mikaelian [13] which does not suffer from the ambiguities of satisfying some higher order boundary conditions. Accordingly we multiply $(31)_1$ by U^m, $(31)_2$ by Θ^m and integrate over the layer to find

$$-Da\langle D^3U\,DU^m\rangle + (2k^2\,Da + 1)\langle DU\,DU^m\rangle + k^2(Da\,k^2 + 1)\langle U\,U^m\rangle + Rc\,k^2\langle(x - x_0)\Theta\,U^m\rangle = 0$$
$$-\langle D\Theta\,D\Theta^m\rangle - (k^2 + Pr\,\sigma)\langle\Theta\,\Theta^m\rangle - \langle U\,\Theta^m\rangle = 0 \tag{33}$$

Here $m = 0$ in the above correspond to moment equations which can be combined into a single equation in Θ as

$$k^2 + Pr\,\sigma - \frac{Rc\,F}{Da\,k^2 + 1} = 0$$

where $F = \frac{\langle(x - x_0)\Theta\rangle}{\langle\Theta\rangle}$. Now equating the imaginary parts of the above equation we find

$$\Im(\sigma) = 0$$

proving the exchange of stabilities irrespective of the nature of the boundary conditions. The principle is therefore valid.

References

[1] P. Vadasz, Stability of free convection in a narrow porous layer subject to rotation, Int. Comm. Heat Mass Transfer 21 (1994) 881–890.
[2] P. Vadasz, Convection and stability in a rotating porous layer with alternating direction of the centrifugal body force, Int. J. Heat Mass Transfer 39 (1996) 1639–1647.
[3] S. Saravanan, H. Yamaguchi, Convection and stability in a magnetic fluid saturated rotating porous layer, in: Proceedings of HT2005, San Francisco, USA, 2005, pp. 17–22.
[4] Om, B.S. Bhadauria, A. Khan, Modulated centrifugal convection in a vertical rotating porous layer distant from the axis of rotation, Transp. Porous Media 79 (2009) 255–264.
[5] J. Serrin, On the stability of viscous fluid motions, Arch. Ration. Mech. Anal. 3 (1959) 1–13.
[6] B. Straughan, The Energy Method, Stability, and Nonlinear Convection, Springer-Verlag, New York, 2004.
[7] B. Straughan, A sharp nonlinear stability threshold in rotating porous convection, Proc. R. Soc. Lond. Ser. A 457 (2001) 87–93.
[8] S. Lombardo, G. Mulone, Necessary and sufficient conditions for global nonlinear stability for rotating double-diffusive convection in a porous medium, Contin. Mech. Thermodyn. 14 (2002) 527–540.
[9] S. Govender, Coriolis effect on the stability of centrifugally driven convection in a rotating anisotropic porous layer subjected to gravity, Transp. Porous Media 67 (2007) 219–227.
[10] D.A. Nield, A. Bejan, Convection in Porous Media, third edition, Springer, New York, 2006.
[11] P.G. Drazin, W.H. Reid, Hydrodynamic Stability, Cambridge University Press, Cambridge, 2004.
[12] B.S. Ng, W.H. Reid, An initial value method for eigenvalue problems using compound matrices, J. Comput. Phys. 30 (1979) 125–136.
[13] Karnig O. Mikaelian, Effect of viscosity on Rayleigh–Taylor and Richtmyer–Meshkov instabilities, Phys. Rev. E 47 (1993) 375–383.